Many-body dynamics of a Bose-Einstein condensate collapsing by quantum tunneling

Hiroki Saito¹

¹Department of Engineering Science, University of Electro-Communications, Tokyo 182-8585, Japan (Dated: July 26, 2017)

The dynamics of a Bose–Einstein condensate of atoms having attractive interactions is studied using quantum many-body simulations. The collapse of the condensate by quantum tunneling is numerically demonstrated and the tunneling rate is calculated. The correlation properties of the quantum many-body state are investigated.

PACS numbers: 03.75.Lm, 03.75.Kk, 67.85.De

I. INTRODUCTION

Attractive interactions between particles destabilize many-body systems against collapse or aggregation. Examples include gravitational collapse of a star and nucleation of drops from supercooled water vapor. Owing to this kind of instability, a dilute Bose gas with attractive interactions cannot form a stable Bose-Einstein condensate (BEC) in an infinite homogeneous system [1]. In a finite system, by contrast, quantum pressure arising from zero-point energies can sustain an attractive force and a metastable BEC can form [2]. Such a metastable BEC with attractive interactions was first realized with trapped ⁷Li atoms [3]. A metastable BEC becomes unstable against collapse when the number of atoms or the scattering length exceeds a critical value [4]. As a result, the number of ⁷Li atoms in the BEC was limited [5]. When atoms are continuously replenished in the BEC, repeated collapse and growth occur [6–9]. The collapse can be investigated in a controlled manner by tuning the interatomic interaction via a Feshbach resonance. The collapsing dynamics of an ⁸⁵Rb BEC has been studied using this technique. The interaction energy is converted into kinetic energy during the collapse, and atomic bursts and jets are produced [10–12]. A Feshbach resonance has also been used to study the amplification of local instabilities [13]. The dynamics of collapsing and exploding BECs have been theoretically investigated by many researchers [14–27].

A trapped metastable BEC with an attractive interaction can collapse by macroscopic quantum tunneling. The tunneling rate can be estimated from an overlap integral [28, 29] or a path integral over the semiclassical trajectory [30–33]. However, the dynamics of a BEC collapsing by quantum tunneling have not been studied. The mean-field approximation, widely used to study BECs, cannot be applied in this situation, because it neglects many-body quantum fluctuations and the metastable state never collapses if the Gross–Pitaevskii equation is used.

In the present paper, direct quantum many-body simulations are preformed to investigate the dynamics of an attractive BEC in a metastable state, and collective quantum many-body collapse by quantum tunneling is demonstrated. Owing to the limited computational re-

source, the system is restricted to a few dozen atoms. The tunneling decay rate is determined for a metastable BEC, and its dependence on the scattering length and on the number of atoms is obtained. It is shown that the quantum state develops into a superposition between metastable and collapsing states.

The paper is organized as follows. Section II formulates the problem and the numerical methods. Section III presents the numerical results. Section IV ends with the conclusions.

II. FORMULATION AND NUMERICAL METHODS

Consider a system of bosonic atoms of mass m confined in an external potential V(r). The interaction between atoms is approximated as a contact potential with an s-wave scattering length a, which is negative for attractive interactions. The Hamiltonian for the system is

$$\hat{H} = \int d\mathbf{r} \hat{\psi}^{\dagger}(\mathbf{r}) \left[-\frac{\hbar^2}{2m} \nabla^2 + V(\mathbf{r}) \right] \hat{\psi}(\mathbf{r}) + \frac{2\pi\hbar^2 a}{m} \int d\mathbf{r} \hat{\psi}^{\dagger 2}(\mathbf{r}) \hat{\psi}^2(\mathbf{r}),$$
(1)

where the field operator $\hat{\psi}(\mathbf{r})$ annihilates an atom located at \mathbf{r} . For simplicity, an isotropic harmonic trap of frequency ω is used,

$$V(\mathbf{r}) = \frac{1}{2}m\omega^2 r^2,\tag{2}$$

where $r^2 = x^2 + y^2 + z^2$.

Although the quantum many-body dynamics will be studied, it is helpful to introduce a mean-field analysis. The Gross–Pitaevskii (GP) equation for the system described by Eq. (1) has the form,

$$i\hbar \frac{\partial \psi}{\partial t} = \left[-\frac{\hbar^2}{2m} \nabla^2 + V(\mathbf{r}) \right] \psi + \frac{4\pi\hbar^2 a(N-1)}{m} |\psi|^2 \psi, \tag{3}$$

where $\psi(\mathbf{r},t)$ is the macroscopic wave function normalized as $\int |\psi|^2 d\mathbf{r} = 1$ and N is the number of atoms. A metastable stationary wave function $\psi_{\rm ms}(r)$ exists [2] for

interaction strengths |g| smaller than a critical value $|g_c|$,

$$g \equiv 4\pi a(N-1)\sqrt{\frac{m\omega}{\hbar}} > g_c \simeq -7.225,$$
 (4)

for an isotropic harmonic trap. When |g| exceeds $|g_c|$, any wave function eventually collapses. On the other hand, when $|g| < |g_c|$, the excitation frequencies above state $\psi_{\rm ms}$ are real and positive, and therefore $\psi_{\rm ms}$ is stable as long as it evolves according Eq. (3). Numerically, a metastable wave function $\psi_{\rm ms}$ can be computed using the imaginary-time propagation method [34], where i on the left-hand side of Eq. (3) is replaced by -1.

Returning to a quantum many-body analysis, the number M of basis functions must be restricted in the numerical calculations. Cut off the field operator as

$$\hat{\psi}(\mathbf{r}) = \sum_{j=1}^{M} \hat{a}_j \phi_j(\mathbf{r}), \tag{5}$$

where \hat{a}_j is the bosonic operator satisfying $[\hat{a}_j, \hat{a}_{j'}^{\dagger}] = \delta_{jj'}$. Using this basis, a many-body state $|\psi\rangle$ can be expanded by Fock states as

$$|\psi\rangle = \sum_{n_1,\dots,n_M} c_{n_1,\dots,n_M} |n_1,\dots,n_M\rangle,$$
 (6)

where

$$|n_1, \cdots, n_M\rangle = \prod_{j=1}^M \frac{(\hat{a}_j^{\dagger})^{n_j}}{\sqrt{n_j!}} |0\rangle \tag{7}$$

with $|0\rangle$ being the vacuum state. The summation in Eq. (6) is over non-negative integers satisfying

$$\sum_{j=1}^{M} n_j = N. \tag{8}$$

Choose the basis functions $\phi_j(\mathbf{r})$ in Eq. (5) as follows. To express the quantum states before collapse, a reasonable choice of basis function is the metastable state of the GP equation:

$$\phi_1(\mathbf{r}) = \psi_{\rm ms}(r). \tag{9}$$

To simulate the collapsing dynamics, in which the state shrinks isotropically, consider functions scaled from $\psi_{\rm ms}(r)$ according to

$$f_j(r) = \psi_{\rm ms}(r/\alpha^j),\tag{10}$$

where $j=2,\cdots,M$ with a constant $0<\alpha<1$. In the numerical calculations presented next, the value of α is taken to lie in the range 0.6-0.7. Using Gram–Schmidt orthonormalization, the other M-1 basis functions are

$$\phi_j(\mathbf{r}) = \mathcal{N}_j \left[f_j(r) - \sum_{n=0}^{j-1} \int \phi_n^*(r) f_j(r) d\mathbf{r} \right], \qquad (11)$$

where \mathcal{N}_j is a normalization factor. Since the collapse occurs isotropically for the potential of Eq. (2), anisotropic quantum fluctuations can be neglected and the basis functions $\phi_j(r)$ can be taken to be isotropic.

Substitution of Eq. (5) into Eq. (1) gives

$$\hat{H} = \sum_{j_1, j_2}^{M} K_{j_1 j_2} \hat{a}_{j_1}^{\dagger} \hat{a}_{j_2} + \sum_{j_1, j_2, j_3, j_4}^{M} I_{j_1 j_2 j_3 j_4} \hat{a}_{j_1}^{\dagger} a_{j_2}^{\dagger} \hat{a}_{j_3} \hat{a}_{j_4},$$
(12)

where

$$K_{j_1 j_2} = \int d\mathbf{r} \phi_{j_1}^*(r) \left[-\frac{\hbar^2}{2m} \nabla^2 + V(\mathbf{r}) \right] \phi_{j_2}(r), \quad (13)$$

and

$$I_{j_1 j_2 j_3 j_4} = \frac{2\pi\hbar^2 a}{m} \int d\mathbf{r} \phi_{j_1}^*(r) \phi_{j_2}^*(r) \phi_{j_3}(r) \phi_{j_4}(r). \quad (14)$$

The number of Fock states in Eq. (7) that satisfy Eq. (8) is

$$n_{\rm F}(N,M) = \frac{(N+M-1)!}{N!(M-1)!}.$$
 (15)

In terms of the Fock basis, the quantum state in Eq. (6) is a vector having $n_{\rm F}$ components and the Hamiltonian is an $n_{\rm F} \times n_{\rm F}$ matrix. The many-body Schrödinger equation,

$$i\hbar \frac{\partial}{\partial t} |\psi(t)\rangle = \hat{H} |\psi(t)\rangle,$$
 (16)

then becomes simultaneous differential equations for the vector of $n_{\rm F}$ components, $c_{n_1,\cdots,n_M}(t)$ in Eq. (6), which are time-integrated using a fourth-order Runge–Kutta method. In the numerical calculations, it is convenient to create a dictionary that provides $\{n_j\}$ given the vector index $\ell=1,\cdots,n_{\rm F}$. To obtain the vector index ℓ from $\{n_i\}$, one can use

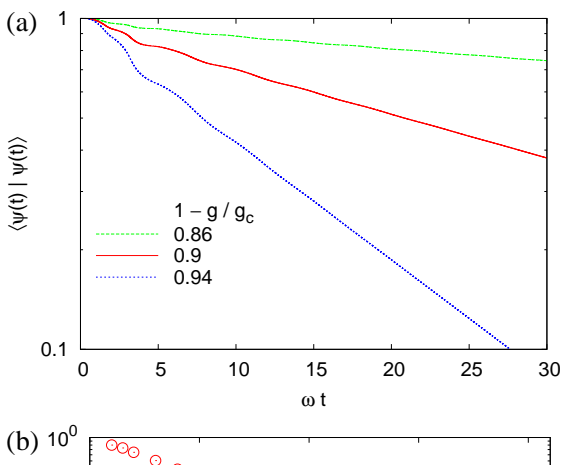
$$\ell = 1 + \sum_{k=1}^{M-1} \binom{N - \sum_{j=1}^{k} n_j + M - k - 1}{M - k}.$$
 (17)

The initial state is taken to be $|N,0,0,\cdots,0\rangle$, i.e., all the atoms occupy wave function $\psi_{\rm ms}(r)$, which is a good starting point for the metastable many-body state. To obtain the decay rate of the metastable state by quantum tunneling, we must identify and eliminate the "collapsed state," which is the portion of the quantum state that has collapsed and never returns to the original state. Since the interaction energy is converted to kinetic energy during the collapse, it is reasonable to assume that the collapsed state consists of Fock states with large kinetic energies. Therefore a non-Hermitian term is added to the Hamiltonian, such as

$$-iL\sum |n_1,\cdots,n_M\rangle\langle n_1,\cdots,n_M|, \qquad (18)$$

where the summation is taken over states satisfying

$$\sum_{j=1}^{M} n_j K_{jj} > E_{\text{threshold}}.$$
 (19)



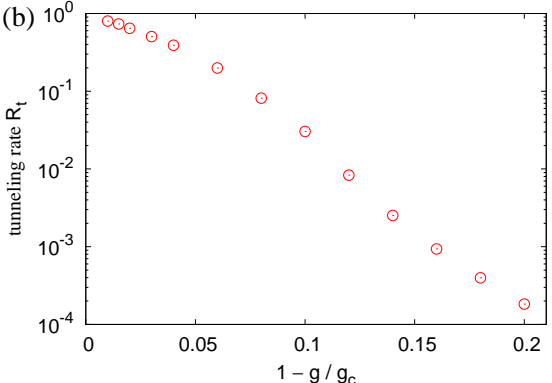


FIG. 1: (color online) (a) Time evolution of $\langle \psi(t)|\psi(t)\rangle$ for $1-g/g_c=0.86$ (dashed line), 0.9 (solid line), and 0.94 (dotted line). (b) Tunneling rate R_t as a function of $1-g/g_c$, where R_t is obtained from the slope of the lines in (a). The number of atoms is N=32 and the number of mode functions is M=6.

Take $L \sim 10\hbar\omega$ and $E_{\rm threshold}$ to be several times larger than NK_{11} . The results hardly depend on these values, implying that the collapsed part of the quantum state is effectively eliminated by this method. If the collapsed portion is left untreated, it bounces back to the original state because of the restricted number of basis functions, and the correct decay rate cannot be obtained.

III. NUMERICAL RESULTS

To demonstrate many-body collapse by quantum tunneling, Eq. (16) is numerically solved for a value of the interaction coefficient g near its critical value g_c . Since the critical value for the collapse is ambiguous in a quantum many-body analysis, the mean-field value g_c in Eq. (4) is adopted as the critical value.

Figure 1(a) plots the time evolution of the norm of the many-body state in Eq. (6),

$$\langle \psi(t)|\psi(t)\rangle = \sum_{n_1,\dots,n_M} |c_{n_1,\dots,n_M}(t)|^2, \qquad (20)$$

which is unity at t=0. For $\omega t\lesssim 1$, $\langle \psi(t)|\psi(t)\rangle$ remains at unity, because it takes a time for the condensate to collapse, as observed in experiments [11]. After $\omega t\sim 1$, a portion of the quantum state undergoes tunneling and collapse, and is removed by the non-Hermitian term in Eq. (18), resulting in the decay of $\langle \psi(t)|\psi(t)\rangle$ seen in Fig. 1(a). For $\omega t\gtrsim 10$, the fluctuations in the curves in Fig. 1(a) attenuate and $\log \langle \psi(t)|\psi(t)\rangle$ decreases linearly in time, indicating that the correct tunneling decay rates are obtained no matter how the initial states are chosen. Define the tunneling rate R_t from

$$\langle \psi(t)|\psi(t)\rangle \sim e^{-R_{\rm t}t},$$
 (21)

obtained from the slope of the lines in Fig. 1(a). Figure 1(b) shows the tunneling rate $R_{\rm t}$ as a function of $1-g/g_{\rm c}$. The tunneling rate $R_{\rm t}$ decreases exponentially with increasing value of $1-g/g_{\rm c}$. However, Fig. 1(b) does not prove whether the tunneling rate obeys $\log R_{\rm t} \propto -(1-g/g_{\rm c})$ [29] or $\log R_{\rm t} \propto -(1-g/g_{\rm c})^{5/4}$ [31, 33]. In these previous studies, the tunneling rate was calculated by the semiclassical approximation valid for a large number of atoms N, whereas the present study only uses a few dozen atoms.

Figure 2(a) plots the dependence of the tunneling rate $R_{\rm t}$ on N, while the value of g in Eq. (4) is fixed at either $0.86g_{\rm c},\,0.9g_{\rm c}$, or $0.94g_{\rm c}$. The tunneling rate $R_{\rm t}$ exponentially decreases with increasing N. The slopes of the lines in Fig. 2(a) are defined as s, i.e.,

$$R_{\rm t} \propto e^{sN}$$
. (22)

The tunneling rate can be estimated by the overlap integral between the mean-field wave functions [29],

$$R_{\rm t} \sim \left| \int \psi_{\rm outside}^*(r) \psi_{\rm ms}(r) d\mathbf{r} \right|^{2N},$$
 (23)

where $\psi_{\rm ms}(r)$ is the metastable wave function and $\psi_{\rm outside}(r)$ is a wave function outside the barrier against collapse. It follows from Eqs. (22) and (23) that $e^{s/2}$ corresponds to the mean-field overlap integral $\left|\int \psi_{\rm outside}^*(r)\psi_{\rm ms}(r)d\boldsymbol{r}\right|$. The values of $e^{s/2}$ and the mean-field overlap integral are plotted in Fig. 2(b). They are seen to be in reasonable agreement. The open circles in Fig. 2(b) lie slightly above the filled circles, probably because there are many paths to collapse other than $\psi_{\rm outside}$.

Before analyzing the properties of the many-body quantum state, consider it qualitatively. Schematically, the quantum state may be written as

$$|\psi_{\text{metastable}}\rangle + |\psi_{\text{collapsing}}\rangle + |\psi_{\text{collapsed}}\rangle,$$
 (24)

where $|\psi_{\rm metastable}\rangle$ is a nearly pure condensate having a Gaussian shape, $|\psi_{\rm collapsing}\rangle$ is a state in which the central density is increasing, and $|\psi_{\rm collapsed}\rangle$ is the state in which the collapse has advanced and the central density has become extremely large or an explosion has

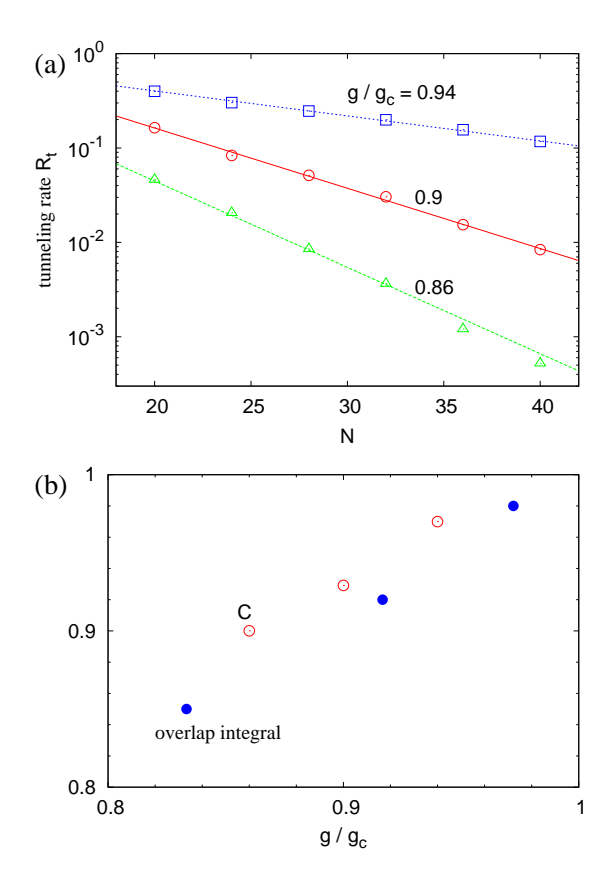


FIG. 2: (color online) (a) Tunneling rate $R_{\rm t}$ as a function of the number of atoms N, where g is fixed at value $0.86g_{\rm c}$ (triangles), $0.9g_{\rm c}$ (circles), and $0.94g_{\rm c}$ (squares). (b) The open circles plot $C=e^{s/2}$, where s is the slope of the lines in (a). The filled circles plot the value of the overlap integral $\left|\int \psi_{\rm outside}^*(r)\psi_{\rm ms}(r)dr\right|$ from Ref. [29]. The number of mode functions is M=6.

occurred. In the present simulation, $|\psi_{\text{collapsed}}\rangle$ is removed by Eq. (18), because it rapidly decoheres from $|\psi_{\text{metastable}}\rangle$ and $|\psi_{\text{collapsing}}\rangle$ owing to the fragility of the macroscopic superposition. Thus the quantum state obtained in the present simulation is written as

$$|\psi\rangle \sim |\psi_{\text{metastable}}\rangle + |\psi_{\text{collapsing}}\rangle.$$
 (25)

Bear in mind that an expectation value is taken with respect to Eq. (25) in the following discussion, not with respect to Eq. (24).

Now consider the density and correlation properties of a quantum many-body state $|\psi\rangle$. The solid curve in Fig. 3(a) plots the expectation value of the atomic density,

$$D(r) = \frac{\langle \psi | \hat{\psi}^{\dagger}(r) \hat{\psi}(r) | \psi \rangle}{\langle \psi | \psi \rangle}.$$
 (26)

The condensate wave function $\chi(r)$ is obtained by diag-

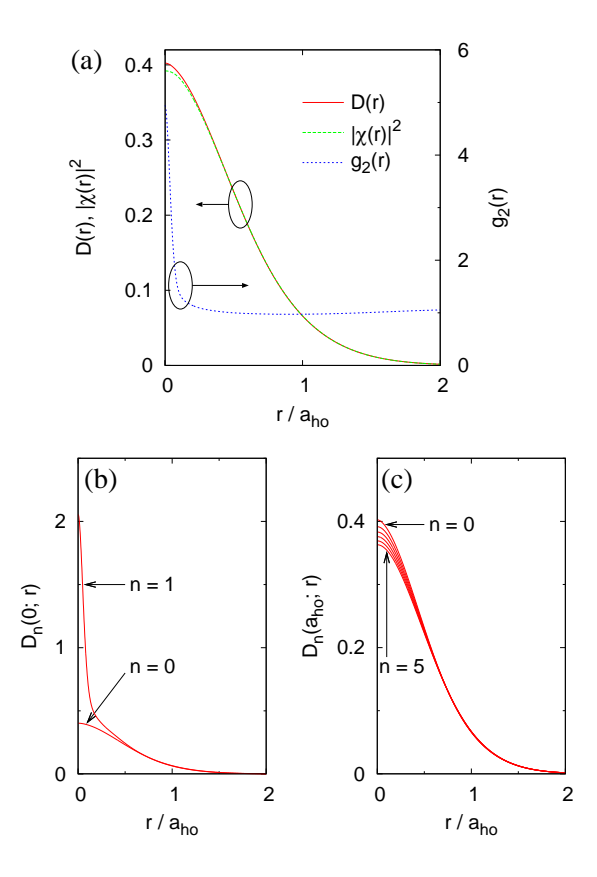


FIG. 3: (color online) (a) Density distribution D(r) from Eq. (26), density $|\chi(r)|^2$ of the condensate wave function from Eq. (28), and the second-order correlation function $g_2(r)$ from Eq. (29). (b)-(c) Conditional density distribution $D_n(r_{\rm d};r)$ from Eq. (30) for (a) $r_{\rm d}=0$ and (b) $r_{\rm d}=a_{\rm ho}$. In (c), $n=0,1,\cdots,5$ from top to bottom. In (a)-(c), the parameters are $g/g_c=0.8,\ N=32$, and M=6. The state $|\psi(t)\rangle$ at $\omega t=30$ is used.

onalizing the single-particle density matrix,

$$\begin{pmatrix}
\langle \hat{a}_{1}^{\dagger} \hat{a}_{1} \rangle & \cdots & \langle \hat{a}_{1}^{\dagger} \hat{a}_{M} \rangle \\
\vdots & \ddots & \vdots \\
\langle \hat{a}_{M}^{\dagger} \hat{a}_{1} \rangle & \cdots & \langle \hat{a}_{M}^{\dagger} \hat{a}_{M} \rangle
\end{pmatrix}.$$
(27)

Using the normalized eigenvector \boldsymbol{v} of this matrix having the largest eigenvalue, the condensate wave function $\chi(r)$ is written as

$$\chi(r) = \sum_{j=1}^{M} v_j \phi_j(r). \tag{28}$$

The density $|\chi(r)|^2$ is shown as the dashed curve in Fig. 3(a), where the condensate fraction is 0.997. For $r/a_{\rm ho} \lesssim 0.2$, the density D(r) deviates from the condensate density $|\chi(r)|^2$. The dotted curve in Fig. 3(a) shows the second-order correlation function

$$g_2(r) = \frac{1}{D^2(r)} \frac{\langle \psi | \hat{\psi}^{\dagger 2}(r) \hat{\psi}^2(r) | \psi \rangle}{\langle \psi | \psi \rangle}, \tag{29}$$

which has a sharp peak at the center, where the density fluctuation is large.

The deviation of D(r) from $|\chi(r)|^2$ and the large peak in $g_2(r)$ at the center of the BEC in Fig. 3(a) arise because the quantum state has the form of Eq. (25). To verify that, the conditional density distribution after natoms are detected at $r = r_d$,

$$D_n(r_d; r) = \mathcal{N}\langle \hat{\psi}^{\dagger n}(r_d) \hat{\psi}^{\dagger}(r) \hat{\psi}(r) \hat{\psi}^{n}(r_d) \rangle, \qquad (30)$$

is calculated, where \mathcal{N} is the factor normalizing $\int D_n(r_{\rm d};r)dr=1$. For example, for a pure condensate, Eq. (30) is independent of n and $r_{\rm d}$: $D_n(r_{\rm d};r)=|\chi(r)|^2$. Figures 3(a) and 3(b) show $D_n(r_{\rm d};r)$ for $r_{\rm d}=0$ and $r_{\rm d}=a_{\rm ho}\equiv [\hbar/(m\omega)]^{1/2}$. If an atom is detected at the center of the trap $(r_{\rm d}=0)$, the state reduction enhances the second term in Eq. (25), resulting in an increase in the central density, as seen in Fig. 3(a). If an atom is detected at the periphery of the cloud, on the other hand, the second term in Eq. (25) reduces, and the density distribution changes as shown in Fig. 3(b). It can thus be concluded that the quantum many-body state evolves to a superposition between a metastable state with a Gaussian-like density distribution and the small fraction of the collective collapsing state having a sharp central density.

For 1 < n < N, the distribution $D_n(r_d = 0; r)$ has a sharp central peak similar to the curve for n = 1 in Fig. 3(a). This fact indicates that the collective collapse dominates the collapsing dynamics, in which $\sim N$ atoms participate in the collapse. If the sharp central peak in $D_n(r_d = 0; r)$ vanished for $n \gtrsim N_1$, it would be regarded as a partial collapse [28], in which a cluster of N_1 atoms collapses and $N - N_1$ atoms remain in the Gaussian-like wave function. However, that does not happen in the present simulation.

IV. CONCLUSIONS

The quantum many-body dynamics have been investigated for a BEC with attractive interactions. A numerical method has been developed that is suitable for simulating the collapsing dynamics. The method was applied to a system of a few dozen atoms to demonstrate the collapse of a BEC by quantum tunneling. This result is the first numerical simulation of a quantum manybody system collapsing upon itself. Due to the quantum tunneling, the uncollapsed component decays exponentially (Fig. 1(a)), so that the tunneling rate can be obtained. The tunneling rate decreases exponentially with an increase in the value of $1 - g/g_c$ (Fig. 1(b)) and of N (Fig. 2(a)). The tunneling rate is in reasonable agreement with the overlap integral computed between the mean-field wave functions before and after the tunneling (Fig. 2(b)). The quantum many-body state develops into a macroscopic superposition between the uncollapsed and collapsing states (Fig. 3).

If the number of mode functions can be increased, then the exploding dynamics can also be studied, revealing the quantum many-body properties of the burst atoms.

Acknowledgments

This work was supported by a Grant-in-Aid for Scientific Research (Nos. 23540464 and 25103007) from the Ministry of Education, Culture, Sports, Science and Technology of Japan.

- H. T. C. Stoof, Phys. Rev. A 49, 3824 (1994).
- [2] P. A. Ruprecht, M. J. Holland, K. Burnett, and M. Edwards, Phys. Rev. A 51, 4704 (1995).
- [3] C. C. Bradley, C. A. Sackett, J. J. Tollett, and R. G. Hulet, Phys. Rev. Lett. 75, 1687 (1995); ibid. 79, 1170 (1997).
- [4] J. L. Roberts, N. R. Claussen, S. L. Cornish, E. A. Donley, E. A. Cornell, and C. E. Wieman, Phys. Rev. Lett. 86, 4211 (2001).
- [5] C. C. Bradley, C. A. Sackett, and R. G. Hulet, Phys. Rev. Lett. 78, 985 (1997).
- [6] Yu. Kagan, A. E. Muryshev, and G. V. Shlyapnikov, Phys. Rev. Lett. 81, 933 (1998).
- [7] C. A. Sackett, H. T. C. Stoof, and R. G. Hulet, Phys. Rev. Lett. 80, 2031 (1998).
- [8] C. A. Sackett, J. M. Gerton, M. Welling, and R. G. Hulet, Phys. Rev. Lett. 82, 876 (1999).
- [9] J. M. Gerton, D. Strekalov, I. Prodan, and R. G. Hulet, Nature (London) 408, 692 (2000).
- [10] S. L. Cornish, N. R. Claussen, J. L. Roberts, E. A. Cornell, and C. E. Wieman, Phys. Rev. Lett. 85, 1795

- (2000).
- [11] E. A. Donley, N. R. Claussen, S. L. Cornish, J. L. Roberts, E. A. Cornell, and C. E. Wieman, Nature (London) 412, 295 (2001).
- [12] P. A. Altin, G. R. Dennis, G. D. McDonald, D. Döring, J. E. Debs, J. D. Close, C. M. Savage, and N. P. Robins, Phys. Rev. A 84, 033632 (2011).
- [13] J. K. Chin, J. M. Vogels, and W. Ketterle, Phys. Rev. Lett. 90, 160405 (2003).
- [14] L. P. Pitaevskii, Phys. Lett. A 221, 14 (1996).
- [15] Yu. Kagan, E. L. Surkov, and G. V. Shlyapnikov, Phys. Rev. Lett. 79, 2604 (1997).
- [16] A. Eleftheriou and K. Huang, Phys. Rev. A 61, 043601 (2000).
- [17] H. Saito and M. Ueda, Phys. Rev. Lett. 86, 1406 (2001);
 Phys. Rev. A 63, 043601 (2001); ibid. 65, 033624 (2002).
- [18] R. A. Duine and H. T. C. Stoof, Phys. Rev. Lett. 86, 2204 (2001).
- [19] V. A. Yurovsky, Phys. Rev. A 65, 033605 (2002).
- [20] L. Santos and G. V. Shlyapnikov, Phys. Rev. A 66, 011602 (2002).

- [21] S. K. Adhikari, Phys. Lett. A 296, 145 (2002); Phys.
 Rev. A 66, 013611 (2002); J. Phys. B 37, 1185 (2004).
- [22] J. N. Milstein, C. Menotti, and M. J. Holland, New J. Phys. 5, 52 (2003)
- [23] C. M. Savage, N. P. Robins, and J. J. Hope, Phys. Rev. A 67, 014304 (2003).
- [24] E. A. Calzetta and B. L. Hu, Phys. Rev. A 68, 043625 (2003).
- [25] S. Métens, G. Dewel, and P. Borckmans, Phys. Rev. A 68, 045601 (2003).
- [26] W. Bao, D. Jaksch, and P. A. Markowich, J. Phys. B 37, 329 (2004).
- [27] S. Wüster, J. J. Hope, and C. M. Savage, Phys. Rev. A 71, 033604 (2005).

- [28] Yu. Kagan, G. V. Shlyapnikov, and J. T. M. Walraven, Phys. Rev. Lett. 76, 2670 (1996).
- [29] E. V. Shuryak, Phys. Rev. A 54, 3151 (1996).
- [30] H. T. C. Stoof, J. Stat. Phys. 87, 1353 (1997).
- [31] M. Ueda and A. J. Leggett, Phys. Rev. Lett. 80, 1576 (1998); X.-B. Wang, L. Chang, and B.-L. Gu, *ibid.* 81, 1342 (1998); M. Ueda and A. J. Leggett, *ibid.* 81,1343 (1998).
- [32] M. Ueda and K. Huang, Phys. Rev. A 60, 3317 (1999).
- [33] C. Huepe, S. Métens, G. Dewel, P. Borckmans, and M. E. Brachet, Phys. Rev. Lett. 82, 1616 (1999).
- [34] F. Dalfovo and S. Stringari, Phys. Rev. A 53, 2477 (1996).